

# CRYOGENIC CURRENT COMPARATOR AS LOW INTENSITY BEAM CURRENT MONITOR IN THE CERN ANTIPROTON DECELERATORS

M. Fernandes\*, The University of Liverpool, U.K. & CERN, Geneva, Switzerland  
 J. Tan, L. Sjøby, CERN, Geneva, Switzerland,  
 C.P. Welsch, Cockcroft Institute & The University of Liverpool, Liverpool, U.K.

## Abstract

In the low-energy Antiproton Decelerator (AD) and the future Extra Low ENergy Antiproton (ELENA) rings at CERN, an absolute measurement of the beam intensity is essential to monitor any losses during the deceleration and cooling phases. However, existing DC current transformers can hardly reach the  $\mu\text{A}$  level, while at the AD and ELENA currents can be as low as 100 nA. A Cryogenic Current Comparator (CCC) based on a superconducting quantum interference device (SQUID) is currently being designed and shall be installed in the AD and ELENA machines. It should meet the following specifications: A current resolution smaller than 10 nA, a dynamic range covering currents between 100 nA and 1 mA, as well as a bandwidth from DC to 1 kHz. Different design options are being considered, including the use of low or high temperature superconductor materials, different CCC shapes and dimensions, different SQUID characteristics, as well as electromagnetic shielding requirements. In this contribution we present first results from a comparative analysis of different monitor options, taking into consideration the external electromagnetic sources at the foreseen device locations.

## LOW-ENERGY ANTIPROTON RINGS AT CERN

The CERN low-energy antiproton physics experiments are currently served by the AD ring. The main purpose of this machine is to capture the antiprotons produced by colliding a proton beam against a fixed target, and then decelerate and cool them to create antiproton bunches suitable to be used by the experiments. ELENA [1] will be a new ring installed downstream of the AD, with the purpose of further decelerating and cooling the antiproton beam.

The goal of the CCC project is to develop a new current monitor to be installed in the ELENA machine, expected to be commissioned in 2016. Before this, the device should be installed and tested in the AD. Both machines have many beam parameters in common. The beam currents in the ELENA are very close to the ones in the AD, since the beam velocity is decreased (from  $\beta = 0.11$  to  $\beta = 0.01$  at lowest energy) by the same order of magnitude as the machine circumference ( $C = 182.5$  m in the AD and  $C = 30.4$  m for the ELENA). In this paper we will focus on the AD machine.

The beam parameters at the different plateau stages of the operation cycle in the AD ring are shown in Table 1.

The beam is injected with  $\beta = 0.97$  containing approximately  $N_p = 5 \times 10^7$  antiprotons. By the end of the cycle the beam is non-relativistic with  $\beta = 0.11$ , and the total intensity normally decreases to  $N_p = 3 \times 10^7$ . The low number of antiprotons combined with low energy regime produces a beam current with the low 300 nA in the case of a final intensity of  $N_p = 1 \times 10^7$ . Figure 1 shows the average current profile during one deceleration cycle assuming a constant number of antiprotons  $N_p = 5 \times 10^7$ .

Table 1: AD Machine Beam Parameters Related to the Different Times in the Cycle Shown in Fig. 1

	A	B	C	D
$\beta$	0.97	0.91	0.30	0.11
$E_K$ [MeV]	2753	1271	46.8	5.3
$f_{\text{rev}}$ [MHz]	1.6	1.5	0.50	0.17
$I_{\text{mean}}$ [ $\mu\text{A}$ ]	12	11	4	1.3 - 0.3
$I_{\text{bunch}}$ [ $\mu\text{A}$ ]	74	140	41	150
$\sigma_{\text{bunch}}$ [ns]	172	136	104	>110

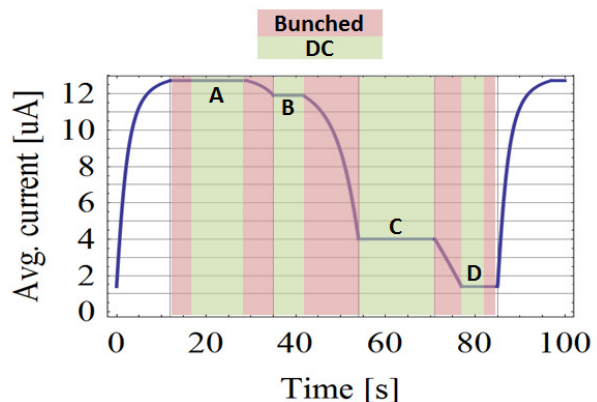


Figure 1: Evolution of the average beam current during one cycle of AD.

The AD is operated with bunched beams during the deceleration phases and with a coasting (DC) beam during the cooling stages, as indicated in figure 1. Measurement of beam intensity is required during both phases.

## Current Monitoring

A precise measurement of the beam intensity in the AD ring is of fundamental importance to monitor the efficiency of the different deceleration and beam cooling phases. Non-perturbing monitors, such as beam DC current

\* Supported by the EU within the oPAC project under contract 289485.

transformers or longitudinal-Schottky pickup noise analysis, rely on sensing the beam-induced electromagnetic field. The DC monitor in particular is limited to a resolution of about  $1 \mu\text{A}$ , normally achieved after an integration period of  $\sim 1 \text{ s}$  [2].

In the AD a direct measurement of beam intensity is available for bunched beams through AC-coupled fast beam current transformers. For the unbunched beam, the intensity cannot be measured by DC Current Transformers (DCCTs) since the beam currents are below the sensitivity of these devices. To overcome this, a system based on the on-line analysis of longitudinal Schottky noise (L-Schottky) was implemented, with the following performance:

- Absolute accuracy error:  $\geq 10\%$
- Time resolution: 200 ms
- Complex calibration procedure

The L-Schottky monitor is also used to measure the bunched beam current. In this case the accuracy and time resolution of the measurement are improved, but another limitation shows up in that the measured current becomes dependent on the longitudinal bunch shape (with accuracy of 5 %, and absolute calibration error of 10 %). Despite its limitations, this monitor has enabled routine operation of the machine over many years. Under the currently ongoing renovation program of the AD beam instrumentation, this system will be renewed leading to small performance improvements [3].

The above limitations prompted us to look for a new type of device for measuring the mean beam current, that could benefit the machine optimization and daily operations.

### Specifications for a More Precise Current Monitor

For a performance breakthrough in the beam current monitoring of the AD machine, a new device should aim to fulfil the following specifications:

- Measurement of absolute mean current of both bunched and coasting beams;
- Easy and accurate calibration procedure using a calibration turn on the toroid;
- Independence of beam shape, trajectory and energy;
- Cover the full range of mean beam current [0.3 – 12]  $\mu\text{A}$ ;
- Current resolution: 3 nA <sup>1</sup>;
- Bandwidth range of [DC – 1] kHz;

The above current resolution is an increase by an order of magnitude over the L-Schottky device, and the increase in bandwidth would represent an improvement by a factor of 200, in the DC mode.

<sup>1</sup>This would permit an accuracy of 1% for the lowest current of 300 nA.

## CRYOGENIC CURRENT COMPARATOR

Cryogenic Current Comparators were first used in electric metrology systems for the precise measurement of DC current ratios [4]. When used to measure a beam current there is a single current, and this is not flowing through a wire. But the working principle is the same as for the current comparison device.

As for any other beam current transformer the CCC relies on measuring the distribution of the magnetic field generated by the circulating beam. A superconductor shielding structure (which in its simplest form is a straight cylinder) surrounding the beam is used to suppress all the magnetic field components that are not linked to the beam current. The resulting magnetic field, which is independent of beam trajectory and energy, needs then to be measured by an extremely sensitive magnetometer. A Superconductor QUantum Interference Device (SQUID) is normally chosen for this task.

In Table 2 a summary is given of the achievable performance with CCC devices and other non-destructive current monitors capable of DC measurement. Two types of CCC, which are discussed in the next sub-sections, are shown depending on the use of Low- or High-Temperature Superconductor (LTS or HTS) materials.

Table 2: Comparison of Different Non-Destructive Current Monitors Capable of DC Measurement

Monitor	Resolution
DCCT	1 $\mu\text{A}$
HTS CCC	100 nA
LTS CCC	8 nA

### Low- vs High- Temperature SC

CCC beam current monitors using both Low- and High-Temperature superconductors have been developed at different institutes. We have reviewed mainly the devices developed at GSI [5] and RIKEN [6]. Although these share many things in common concerning their working principle, there are some important differences.

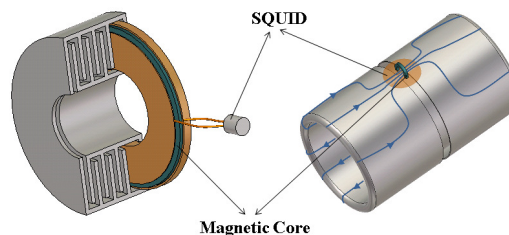


Figure 2: Schematic of two different CCC systems. On the left is a LTS version and on the right is a HTS one.

High-temperature superconductors available today are ceramic materials that are hard to manufacture into com-

plex shapes. In addition it is difficult to connect superconducting wires. Given these limitations the HTS CCC devices developed to date are based on a straight cylindrical tube of superconductor for shielding, with the SQUID sensor located directly on top of the cylinder as shown in figure 2. To maximise the coupling of the magnetic field created by the mirror current to the sensor, a superconductor bridge pattern is created in order to concentrate the total current under the SQUID pickup coil, which is normally used in a gradiometer configuration. A small ferromagnetic core can also be used to increase the magnetic flux in the SQUID pickup coil. However, problems due to the finite length of the shielding tube, shielding from external sources and insufficient magnetic coupling to the SQUID detector, still limit the performance of these devices when compared with the LTS version [6].

In the LTS version of the CCC a meander-shaped shielding has been proposed that allows for reducing the total length, when compared to a simple cylinder, and at the same time acts as a shield against noisy background magnetic field, see figure 2. A small gap opening is needed to allow for the beam magnetic field to enter into the cavity where a high magnetic permeability core is located with a single turn secondary coil that is used to couple the magnetic field to a SQUID outside of the cavity.

The LTS CCC devices developed to date were able to achieve a higher resolution than the HTS ones, as can be seen in Table 2. The system developed by A.Peters *et al.* with 8 nA resolution<sup>2</sup> would be close to fulfilling the specifications of the AD/ELENA device.

### Challenges and Future R&D Topics

The beam pipe aperture at the location foreseen for the installation of the LTS CCC is 160 mm. But, the AD machine optics has changed considerably over the years and the aperture required for the new diagnostics is only between 100 – 110 mm. Taking into account the additional space needed for a cryostat isolation around the beam pipe, the magnetic core radius should be around  $r_{MC} = 80$  mm. The smallest beam current that we want to measure is  $0.3 \mu\text{A}$ , which at  $r_{MC}$  creates a magnetic field of  $\sim 0.75$  pT, compared to the Earth’s magnetic field on the order of  $50$ ’s  $\mu\text{T}$ . In order to keep the 1% accuracy, the shielding should provide for an attenuation factor of 200 dB. Other groups have reported attenuation factors for LTS CCC shielding structure close to this value [7], and so shielding should not be a problem.

Apart from the shielding, the CCC resolution will depend on different factors that can be optimized. Other groups have carried intensive research into the optimization of the different components of the system that limit the overall system resolution [8].

Nowadays, low-noise DC SQUIDS may achieve an input sensitivity of the order of  $0.23 \mu\text{A}/\phi_0$  (where  $\phi_0$  is the magnetic flux quantum constant<sup>3</sup>) with a typical white

noise density of  $1.2 \mu\phi_0/\sqrt{\text{Hz}}$ , corresponding to a current noise of  $0.28 \text{ pA}/\sqrt{\text{Hz}}$ . The indicated values are for a DC SQUID device [9] manufactured by Magnicon GmbH. The current SQUID control electronics exhibit comparable noise figures, and none of these two components limit the system resolution.

The dominant intrinsic noise source is in the magnetic coupling circuit. In order to maximize the S/N ratio a high inductance soft ferromagnetic core in the pickup coil is used. Studies of different materials [10] have shown that nanocrystalline materials, such as Nanoperm M-764-01, exhibit the best noise performance at liquid Helium temperatures (below 4.2 K).

Additional noise contributions, and also possible sources of a zero-drift current, are disturbing magnetic background fields, mechanical vibrations and temperature variations of the SQUID. Study of different techniques to overcome these will be our main research topic.

Another issue with the implementation of a CCC at the AD and ELENA is the sharp increase in the magnetic field during the bunched beam phases (bunch lengths  $\sim 100$  ns). The SQUID electronic system working in Flux-Locked Mode cannot keep track of signals varying at rates exceeding its slew-rate, which is typically of the order of  $15 \text{ M}\phi_0/\text{s}$ . This is insufficient for the bunched beam structure in AD and ELENA, where, depending on cross section of the magnetic core and single-turn pickup coil, the flux variation could be of the order of  $100 \text{ M}\phi_0/\text{s}$  or even  $1000 \text{ M}\phi_0/\text{s}$ . We are currently studying possible solutions to this problem. One possibility would be to profit from a possible low-pass filtering effect in the shielding structure. Another option would be to use metallized ceramic gaps in the beam pipe to minimise the higher frequency components seen by the CCC.

## MAGNETIC ENVIRONMENT

Different magnetic noise sources near the CCC have been measured or estimated: Modelling of the Earth’s magnetic field; Measurements of magnetic field inside the AD hall; Simulation of stray fields from nearby magnets.

The Earth’s magnetic field in the Geneva region has a magnitude of  $47 \mu\text{T}$ , with a vertical component of  $42 \mu\text{T}$  and an horizontal component of  $22 \mu\text{T}$  [11]. The daily and yearly variation is under 1%.

Measurements of the magnetic field at different points inside the AD hall have been performed by the CERN Magnetic Measurements section. The overall background field level is  $< 10 \mu\text{T}$  at places away from magnetic flux concentration points such as crane equipment.

As can be seen from figure 3 the two closest magnet elements are two focusing and defocusing quadrupoles located 1600 mm away from the mid-point of the proposed CCC location, named QDS15 and QFN16. In order to estimate the stray fields, we performed magnetostatic simulations of these two elements using the software CST EM Studio. The models created replicate the real iron core, the poles shape, and the quadrupole coils (QDS15 coils have

<sup>2</sup>Achieved current noise density of  $250 \text{ pA}/\sqrt{\text{Hz}}$ .

<sup>3</sup> $\phi_0 = \frac{h}{2e} = 2.067834 \times 10^{-15} \text{ Wb}$

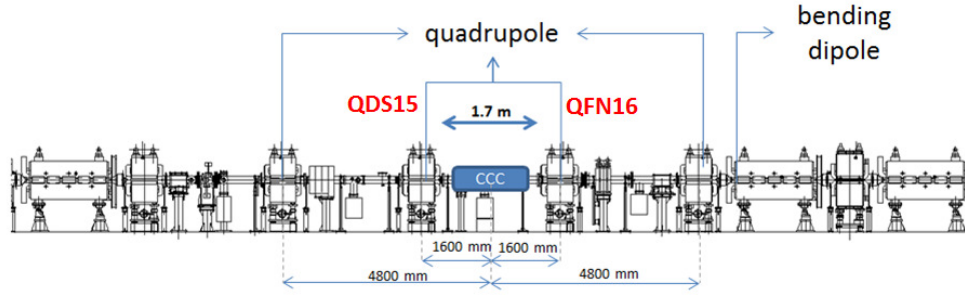


Figure 3: Location of the CCC in the AD ring.

17 turns, while QFN16 ones have 19). The currents used to feed the magnet windings was  $I_{\text{Quad}} = 2005 \text{ A}$ , corresponding to the maximum field plateau (phase A in Table 1).

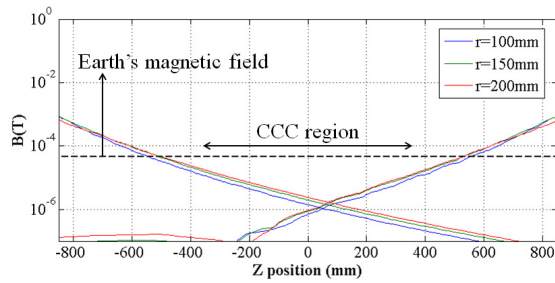


Figure 4: Absolute value of the transverse component of the magnetic field from the quadrupoles.

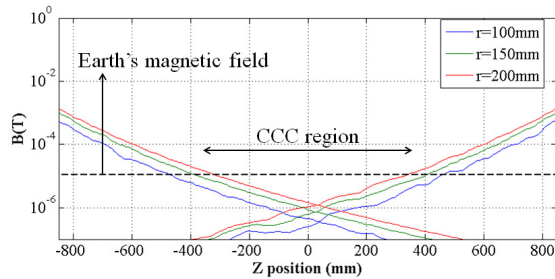


Figure 5: Absolute value of the longitudinal component of the magnetic field from the quadrupoles.

In figures 4 and 5 we present the magnitude of transverse and longitudinal magnetic fields in the XZ plane rotated by  $45^\circ$  around the Z axis, at different radius values. This is the plane where the longitudinal components of the magnetic field is maximum, while the transverse component has approximately the same magnitude as in the XZ plane. The Z axis origin is located mid-way between QDS15 and QFN16, at the probable location for the CCC device that should have a length  $< 1 \text{ m}$  including the cryostat.

We verify that in the the region  $|z| < 1 \text{ m}$ , both the transverse and longitudinal components of the stray magnetic fields are  $< 0.1 \mu\text{T}$ . And in almost all the extent of this region are below the corresponding Earth's magnetic field component in the same location.

## CONCLUSIONS

By comparing the requirements for an improved beam current monitor for the low-energy antiproton rings AD and ELENA with existing current monitors we conclude that the LTS CCC is the only device capable of achieving the required current resolution of  $3 \text{ nA}$ . After fixing the desired specifications, we assessed the background magnetic field in the AD and found that the simulated stray fields induced by the nearest magnet elements in the previewed region for the CCC are below the Earth's magnetic field.

## ACKNOWLEDGMENT

I would like to thank Marco Buzio (CERN) for the results of the magnetic measurement inside the AD hall, and GSI colleagues for fruitful discussions. As well as acknowledgement oPAC network support.

## REFERENCES

- [1] T. Eriksson, *et al.*, "The Elena project: Progress in the design", THPPP008, Proceedings of IPAC2012.
- [2] P. Odier, "DCCT technology review," C04-12-01.1, Proceedings of CARE-HHH-ABI.
- [3] M. Ludwig, "Beam instrumentation and electron cooling needs for the AD in the ELENA era," Functional Specification, CERN, Switzerland, October 2012.
- [4] I.K. Harvey, *Rev. Sci. Instrum.* 43 (1972) 1626.
- [5] A. Peters, *et al.*, *Journal of Physics: Conference Series* 43 (2006) 1215.
- [6] T. Watanabe, *et al.*, "Improvement of beam current monitor with high  $T_c$  current sensor and SQUID at the RIBF," TUPC105, Proceedings of IPAC2011.
- [7] F. Kurian, *et al.*, "Field attenuation of the magnetic shield for a Cryogenic Current Comparator," MOPGR001, Proceedings of BIW2012.
- [8] R. Geithner, *et al.*, "An improved Cryogenic Current Comparator for FAIR," MOPPR020, Proceedings of IPAC2012.
- [9] [http://www.magnicon.com/fileadmin/download/datasheets/Magnicon\\_Squids.pdf](http://www.magnicon.com/fileadmin/download/datasheets/Magnicon_Squids.pdf)
- [10] A. Steppke, *et al.*, *IEEE Trans. on Applied Superconductivity*, 19-3 (2009) 768.
- [11] British Geological Survey, <http://www.geomag.bgs.ac.uk>